Title

Origins and demonstrations of electrons with orbital angular momentum

Journal

Philosophical Transactions of the Royal Society A Mathematical Physical and Engineering Sciences, 375(2087)

ISSN

1364-503X

Authors

McMorran, Benjamin J

Agrawal, Amit

Ercius, Peter A

et al.

Publication Date

2017-02-28

DOI

10.1098/rsta.2015.0434

Peer reviewed

PHILOSOPHICAL TRANSACTIONS A

rsta.royalsocietypublishing.org

Research

Cite this article: McMorran BJ, Agrawal A, Ercius PA, Grillo V, Herzing AA, Harvey TR, Linck M, Pierce JS. 2017 Origins and demonstrations of electrons with orbital angular momentum. *Phil. Trans. R. Soc. A* **375**: 20150434. http://dx.doi.org/10.1098/rsta.2015.0434

Accepted: 28 October 2016

One contribution of 14 to a theme issue 'Optical orbital angular momentum'.

Subject Areas:
electron microscopy, optics, quantum physics, wave motion

Keywords:
optical angular momentum, electron vortex, matter wave interferometry

Author for correspondence:
Benjamin J. McMorran
e-mail: mcmorran@uoregon.edu

Electronic supplementary material is available online at https://dx.doi.org/10.6084/m9.figshare.c.3647705.

THE ROYAL SOCIETY PUBLISHING

Origins and demonstrations of electrons with orbital angular momentum

Benjamin J. McMorran[1], Amit Agrawal[2,4], Peter A. Ercius[5], Vincenzo Grillo[1,6], Andrew A. Herzing[3], Tyler R. Harvey[1], Martin Linck[7] and Jordan S. Pierce[1]

[1]Department of Physics, University of Oregon, Eugene, OR, USA
[2]Center for Nanoscale Science and Technology, and [3]Materials Measurement Laboratory, National Institute of Standards Technology, Gaithersburg, MD 20899, USA
[4]Maryland NanoCenter, University of Maryland, College Park, MD 20742, USA
[5]National Center for Electron Microscopy, Molecular Foundry, Lawrence Berkeley National Laboratory, 1 Cyclotron Road, Berkeley, CA 94720, USA
[6]CNR-Istituto Nanoscienze, Centro S3, Via G. Campi 213/a, 41125 Modena, Italy
[7]Corrected Electron Optical Systems GmbH, Englerstraße 28, 69126 Heidelberg, Germany

MB, 0000-0001-7207-1076

The surprising message of Allen *et al.* (Allen *et al.* 1992 *Phys. Rev. A* **45**, 8185 (doi:10.1103/PhysRevA.45.8185)) was that photons could possess orbital angular momentum in free space, which subsequently launched advancements in optical manipulation, microscopy, quantum optics, communications, many more fields. It has recently been shown that this result also applies to quantum mechanical wave functions describing massive particles (matter waves). This article discusses how electron wave functions can be imprinted with quantized phase vortices in analogous ways to twisted light, demonstrating that charged particles with non-zero rest mass can possess orbital angular momentum in free space. With Allen *et al.* as

a bridge, connections are made between this recent work in electron vortex wave functions and much earlier works, extending a 175 year old tradition in matter wave vortices.

This article is part of the themed issue 'Optical orbital angular momentum'.

1. Introduction

(a) A quantum vortex model of matter

The work of Allen *et al.* [1] can be interpreted as a crucial link in a chain of thought extending to a much earlier hypothesis of a vortex nature to matter. One of the earliest reported observations of phase singularities in a wave system was made by Whewell in his study of the tides in the 1830s [2,3] and discussions in a modern context in [4,5]. In 1850, William Rankine presented a paper titled 'Hypothesis of molecular vortices' to the Royal Society of Edinburgh [6]. This inspired further work by Lord Kelvin (William Thomson), who supposed that atoms could be described as knots of vortices in the aether [7]. J. J. Thomson (no relation to Lord Kelvin) developed this idea further by analysing interactions between intertwined vortices of matter [8]. After the discovery of the electron by J. J. Thomson himself, a finding for which he ultimately won the 1906 Nobel Prize in physics [9], he and others abandoned the vortex theory of matter. However, the general idea that particles (and electrons in particular) could have a vortex structure, and an associated angular momentum and azimuthal phase, continued to play an important role in twentieth century physics and beyond. The relatively recent experimental demonstrations of free electron vortex states [10–12] thus represent a continuation of a centuries-old idea. However, whereas the original vortex model of matter was developed to describe the internal structure and behaviour of atoms, these recent demonstrations of electron vortex states occur in freely propagating electron wave functions.

Not long after J. J. Thomson's discovery of the electron, his son, George Paget Thomson, demonstrated the wave-like nature of electrons by diffracting cathode rays from a thin crystal [13], a finding that earned him the 1937 Nobel Prize [14]. The son's discovery that electrons could behave like a delocalized fluid re-opened the door to the elder Thomson's vortex theory of matter. Paul Dirac considered that an electron wave function scattering from a theoretical magnetic charge (magnetic monopole) would acquire an azimuthal phase [15,16]. In order for the scattered electron wave function to not be multivalued, Dirac argued that the amplitude must vanish along a nodal line, and that the azimuthal phase about this singularity must be quantized, thus continuing the thoughts of Thomson, Kelvin and Rankine. With these considerations, Dirac was able to derive a theoretical value of a magnetic monopole quantum in terms of the electron charge e, the speed of light and Planck's constant $\hbar$. Tonomura and colleagues [17,18] proposed the use of electron holography (electron matter wave interferometry) to detect magnetic monopoles, describing the spiral electron wavefront topology and telltale forked interference fringes that would result from a scattering event with a monopole. While Dirac specifically considered quantized electron vortex lines terminated by magnetic monopoles, his consideration of quantized circulation led to a more general understanding of quantum vortices in a greater variety of physical systems.

A quantum vortex is a de Broglie wave function that has non-trivial topology; a vortex state cannot be continuously deformed into a different vortex state without introducing another dislocation in the fluid or wave function. At the vortex core, along the nodal line, the phase of the wave function is undefined and the amplitude is zero. The quantum vortex can be defined by a spatial wave function that includes an azimuthal phase factor, $\exp(\mathrm{i}\ell\phi)$, where integer ℓ is the topological charge of the spiral phase singularity and ϕ is the polar angle about the axis of the phase singularity. From this it can be seen that such quantum vortex wave functions are orbital angular momentum eigenstates, with $\hat{L}_z\psi_\ell = -\mathrm{i}\hbar\partial_\phi\psi_\ell = \ell\hbar\psi_\ell$. Quantum vortices have been observed in a variety of quantum material systems; first in superfluid helium [19], then flux vortices in type II superconductors [20] and on to Bose–Einstein condensates [21]. In the 1970s, Hirschfelder and colleagues conducted a wider study of phase singularities in matter-wave

systems, noting that quantized vortices seem to be an intrinsic property of many physical systems [22,23]. The related concepts of wave function vortices, topology and angular momentum have become central to many modern topics in condensed matter physics and many-particle physics.

Several theoretical works proposed vortex solutions in freely propagating wave fields, too. Nye & Berry [24] developed a theory of phase dislocations and singularities in general wave fields, and later analysed electron 'whirling wave' solutions [25]. Bialynicki-Birula *et al.* [26] predicted the presence of quantum vortex states in particle wave functions and theoretically studied their motion.

In 1992, Allen *et al.* [1] pointed out that photons could also be prepared in quantum vortex states, opening an accessible path to quantum vortices in freely propagating single-particle systems (photons). Commonly referred to as 'optical vortex beams', 'twisted light' or optical orbital angular momentum (OAM), these photon angular momentum states have enabled many advances in a variety of fields within optics, as reviewed elsewhere in this issue. That similar optical vortex states could also be applied to matter waves only became obvious after parallel advances in the unrelated fields of coherent electron microscopy and matter wave optics. Bliokh *et al.* predicted phase vortex states for free electrons [27] and considered their relativistic propagation dynamics.

(b) Original works in free electron vortices

In the 1950s, Suzuki & Willis [28,29] discovered that an azimuthal phase could be generated in an optical field by diffraction from forked structures [28,29]. Notably, Suzuki and Willis were interested in understanding electron and X-ray diffraction from edge dislocations in crystals—i.e. forked periodic structures. To model this, they conducted optical experiments with beams of light using a Lipson diffractometer. They produced an optical mask model of crystal edge dislocations, a two-dimensional array of holes with a dislocation in the centre. When they diffracted coherent light from the structure, they observed dark spots in the diffracted beams, which we now know are due to phase vortices. In [28], Willis reviews Suzuki's theoretical model of the wave function giving rise to the dark spots. Indeed, Suzuki had apparently posited that the wave field possesses a spiral phase singularity, though he did not apparently publish this result himself. Their work is reproduced in figure 1, along with an equivalent demonstration of electron vortices, as they originally envisaged.

Recently, researchers demonstrated that freely propagating electrons can similarly be prepared in quantum vortex states [10–12]. Whereas Tonomura had earlier proposed to detect magnetic monopoles by measuring phase vortices in electron beams [17,18], the work of Allen *et al.* and ensuing discoveries and applications of optical OAM led Uchida & Tonomura [10] to study electron phase vortices themselves. In this work, they constructed a three-level spiral phase plate for electrons using thin plates of graphite, and demonstrated that electrons passed through this stack acquired an azimuthal phase profile, measured by electron holography. At the same time, two other groups working independently had similar interests in free electron vortex states. Verbeeck *et al.* [11] demonstrated quantized electron vortices using diffraction from a microfabricated platinum grating with a fork dislocation, and even performed preliminary explorations of how such states might transfer OAM with matter. Similarly, the author produced nanoscale diffraction holograms with a fork dislocation [30] to efficiently produce electron vortex beams with high OAM [12], demonstrating that even free electron vortex states with much larger amounts of OAM are apparently stable upon propagation.

Similar to an optical vortex, the electron vortex is remarkable for its spiral phase singularity and associated quantized OAM. Yet unlike photon OAM, electrons possess both charge and rest mass. Thus, these demonstrations of free electron vortices were the first experimental observations of single, non-interacting massive particle wave functions occupying vortex states. The electric charge of these OAM states imparts a magnetic moment, such that electron vortices can interact with magnetic fields [31–34] and quantum systems [35–39] in new ways compared

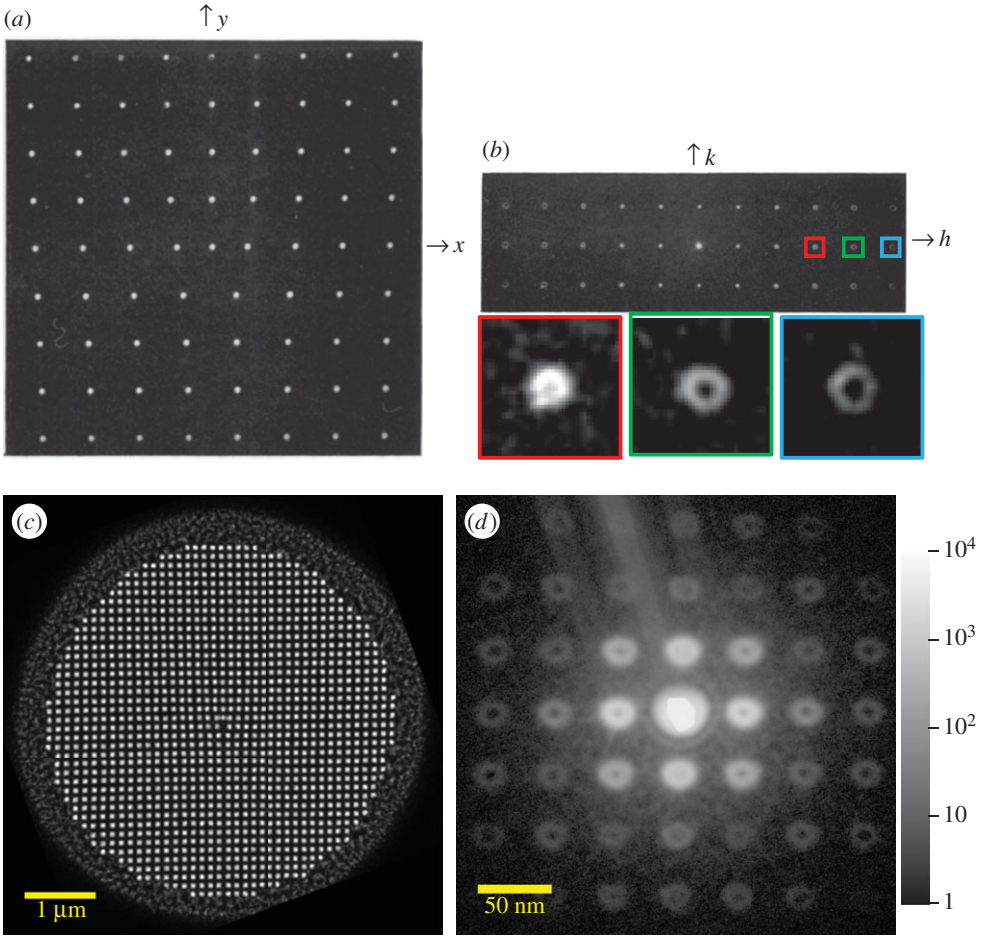

Figure 1. Early work on optical diffraction (*a,b*) from two-dimensional masks is reproducible with electron diffraction (*c,d*). (*a*) An optical mask produced by Willis (adapted from [28]) simulates a natural crystal edge dislocation, with a topological charge of 1 in the *x* direction and 0 in the *y* direction. (*b*) Light diffracted by this mask produces optical vortices (figure adapted from [28]). Here the (0, 3), (0, 4) and (0, 5) diffraction spots corresponding to optical vortices with $\ell = 3$, 4 and 5, respectively, have been enlarged to reveal the central dark spots characteristic of topological charge. (*c*) A nanofabricated two-dimensional grating for electrons simulates an edge dislocation in a single crystal lattice plane. (*d*) The resulting electron diffraction pattern forms a two-dimensional array of electron vortices. In this diffraction image (300 keV, $\lambda = 1.97$ pm), the diffraction spots were defocused in order to enlarge the diffraction spots.

with photon OAM. Furthermore, the de Broglie wavelength of electrons ($\lambda = 1.97$ pm in the case of 300 keV electrons) is much shorter than for experimentally accessible photons, and provides a means of exploring OAM effects at much smaller length scales. These unique properties of the electron vortices will be discussed here.

The outline of this paper is as follows: the key experimental components needed for observations of electron vortices—a coherent electron beam system and singular electron optical elements—will first be discussed in §2. Experimental demonstrations of electron vortex beams with OAM will be presented in §3, followed by a model of such states and a discussion of their magnetic properties in §4.

2. Coherent electron optics

A schematic of the experiments discussed here is shown in figure 2. The recent experimental work with electron vortex beams is enabled by two technologies: (i) improvements in high-resolution

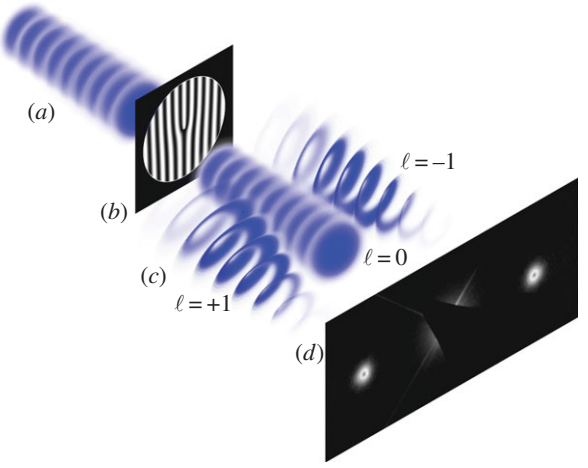

Figure 2. Schematic of electron vortices produced from a diffraction hologram. A spatially coherent electron wave function (*a*) illuminates a nanofabricated forked diffraction grating (*b*). The resulting diffracted portions of the wave function (*c*) possess quantized phase vortices. This diffraction pattern from many non-interacting electrons being diffracted is imaged in an electron microscope (*d*). For the experimental image adapted for (*d*), the undiffracted 0-order beam was blocked by a beam stop.

transmission electron microscopy and (ii) electron wavefront engineering using nanofabricated optics.

(a) Transmission electron microscope: a coherent electron optics bench

Many of the tools necessary for experiments in coherent electron optics are provided in a modern transmission electron microscope (TEM). State-of-the-art aberration-corrected TEMs provide a bright source of coherent electrons in the field emission gun (FEG; the electron analogue to a tunable laser). The electron optics within the TEM provide a versatile system for coherent electron experiments, consisting of several solenoidal magnetic lenses (the electron analogue to high-precision spherical lenses), electrostatic and magnetic multipole lens elements, deflectors, adjustable apertures, multi-axis automated stages with sub-micron positioning accuracy, high-speed single pixel detectors (the equivalent of a photodiode) and imaging detectors (CCDs with scintillators) with high quantum efficiency and high dynamic range. Some TEMs are also equipped with an electrostatic beamsplitter for interferometry/holography, energy spectrometer. Thus, a modern TEM provides the elements necessary for many experiments with coherent electron matter waves.

The electron beams supplied by a TEM equipped with a FEG are analogous to a low-intensity laser in terms of both transverse and longitudinal spatial coherence. While there is no predictable phase relationship between consecutive electrons due to the stochastic nature of the emission process, the very small source size and beam-defining optics result in a high degree of transverse (spatial) coherence. The transverse coherence width of the electron can be large; nearly as large as the width of the beam, which can vary from 0.1 nm to 1 mm. The energy spread of the beam ($\Delta E \approx 0.4$ eV) and the accelerating voltage (typically $E = 300$ keV) results in a longitudinal coherence length for the electrons of only approximately 2 µm. While this longitudinal coherence length (and associated coherence time) is quite short compared with that of lasers, note that this coherence length is quite long compared with the electron de Broglie wavelength ($\lambda = 1.97$ pm). The *relative* longitudinal coherence of electrons in the TEM, defined as the ratio of the coherence length to the de Broglie wavelength, is on the order of 10^6—comparable with a typical HeNe laser. Thus, for the studies of electron OAM presented here, it is reasonable to model the electron wave functions as being monochromatic.

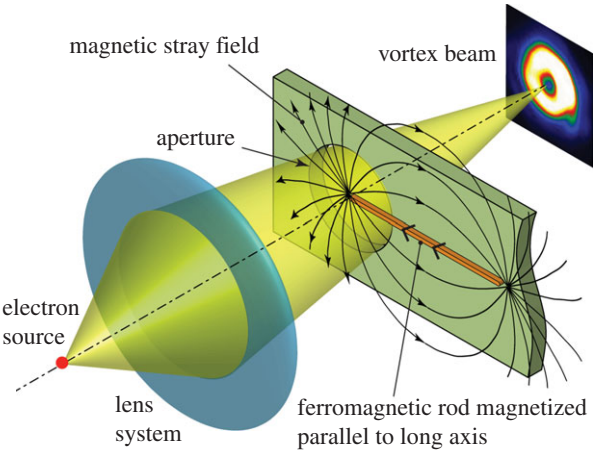

Figure 3. Illustration of the creation of an electron vortex from the monopole-like magnetic field (black lines) of a ferromagnetic rod. The rod is in a plane perpendicular to the elecron optic axis, with one end placed on the optic axis. The field inside the needle strongly deviates from that of a monopole, but the material of the rod is sufficiently thick to scatter out of the optical system electrons that would be otherwise sensitive to the field there. Figure courtesy of Arthur Blackburn.

It should also be noted that, the experiments described here probe single-electron physics. To a good approximation, the electrons in the TEM beam are both (i) non-interacting, and (ii) prepared identically. It is only near the field emission tip that the density of electrons is large enough for mutual Coulomb interactions comes in to play, yet even here the phase-space packing density of electrons is quite low. After the electrons are accelerated to 300 keV, they are separated by an average distance on the order of 10 cm apart along the beam path, even when using a high beam current of 100 pA. This average spacing is too diffuse for multiple electrons to interact. The high degree of transverse spatial coherence of the beam means that electrons are prepared with nearly identical transverse wave functions. In a typical experiment, an imaging detector measures the probability distribution of an ensemble of a great many identically prepared electrons. Thus, the digital images presented here, to a reasonable approximation, represent the probability distribution of a single electron.

(b) Singular electron optics

Conceptually, there is little difference between the physics of engineering the phase of a photon and that of a particle wave function. Electron vortices are prepared using a new class of singular optics for charged particles. Spiral phase plates for electrons—either material [10] or magnetic [40,41]—can be used to directly imprint an azimuthal phase onto an electron beam. Interestingly, the magnetic spiral phase plate concept approximates the same scattering from a magnetic monopole that Dirac studied [15,16]. Because the search for genuine magnetic monopoles is ongoing [42], researchers have instead noticed that the field near the end of an ideal long, thin ferromagnetic rod looks monopole-like and the deviations from a true monopole field are hidden inside the electron-opaque rod. A schematic of the optical system to produce electron vortices with a ferromagnetic rod is shown in figure 3. As with singular optics for light, spiral phase plates are challenging to fabricate, and extreme precision is necessary to imprint a precisely quantized spiral phase onto an electron wave function using these devices [43,44]. Unless a precisely controlled single quantum of magnetic flux emerges from the tip of the magnetic rod, magnetic spiral phase plates will imprint a 'seam' or step in the phase along a radius away from the central vortex, resulting in fractional OAM that is not stable upon propagation [45]. Magnetic rod-based phase plates also become saturated in the external field of a magnetic lens, such as is the case when using them in conventional

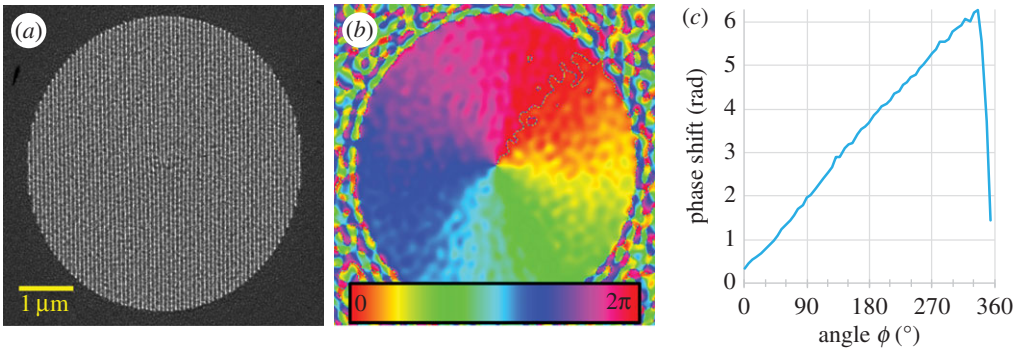

Figure 4. (*a*) A TEM micrograph image of a silicon nitride forked diffraction grating used to imprint spiral phase onto electron beams. The lighter lines are grooves etched partially through the silicon nitride membrane using focused ion beam (FIB) milling, and have a spatial periodicity of 76 nm. (*b*) The fork in the diffraction grating encodes an azimuthally varying spatial phase (represented by colour scale) in the lateral registration of the grooves, revealed here by Fourier-filtering the TEM micrograph image in (*a*). (*c*) A radially averaged plot of the phase in (*b*) shows that it varies smoothly and linearly as a function of the polar angle ϕ and wraps continuously to 2π. In an actual electron diffraction experiment, this spiral phase is imprinted onto the $+1$ diffraction order, and the opposite winding direction is imprinted onto the -1 diffraction order.

aperture locations within an electron microscope. However, two groups working independently are making advances in the design, fabrication and use of these devices [40,41]. Vortex beams can also be produced with electrostatic rod-based spiral phase plates; such a rod could be used in the high magnetic field of a lens [46] (RE Dunin-Borkowski 2016, personal communication).

Diffraction holograms provide an alternative means of precisely imprinting OAM in all types of matter waves—not just electrons. Similar to gratings used in light optics [47–49], electron vortices can be produced by diffraction from nanoscale holographic gratings featuring a fork dislocation [11,12,30] (figure 2). As in optics, the dislocation at the centre of a forked grating encodes a spiral phase. This spiral phase can be revealed by Fourier-filtering the spatial components of an image of the grating, as shown in figure 4. The number of extra grooves present in the grating determines the topological charge (winding number) of the spiral phase. The lateral nanoscale position of lines (actually grooves) within the grating pattern determines the *picometre* shift in the phase of the electron de Broglie wave. Thus, the overall size of the patterned area, the resolution with which the line features can be placed and the spatial coherence of an array of such lines are all factors of the hologram design.

Electron diffraction holograms must have an extremely small average spatial period (lattice spacing) between lines in order to provide sufficient angular separation between diffracted electron beams. This can be achieved using modern nanofabrication techniques, such as e-beam lithography (EBL) [50,51] or focused ion beam (FIB) milling [12,30,52] to create holes prescribed depth in a silicon nitride membrane. These methods are used to produce the electron diffraction holograms shown in this paper, with spatial periodicities (pitch) between 50 nm and 100 nm. These gratings provide an angular separation between diffracted 300 keV electrons of 39 µrad to 20 µrad, respectively, which is sufficient for use in a TEM.

Silicon nitride is suitable for nanoscale diffractive optics for electrons because it is mechanically strong, does not melt under exposure to an intense electron beam, and it is transparent to electrons which, as will be discussed, is important for use in efficient *phase gratings* and interferometry. We find that these structures can be used over the course of several months in a TEM. With prolonged exposure to an electron beam under non-ideal vacuum conditions, the diffraction gratings can get contaminated due to carbon deposition, which decreases their diffraction efficiency and introduces unwanted phase distortions in the beam. Plasma cleaning the gratings restores their original functionality.

A major challenge with diffractive electron optics is that only a fraction of the electron beam incident on a grating gets diffracted into a desired diffraction order. The diffraction efficiency of a grating, defined as the beam current in a desired diffraction order relative to the beam current incident on the grating, thus becomes a major concern for use in an electron microscope, where experiments are often starved for signal. Whereas our early nanofabricated forked holograms [30] served as binary masks for low-energy electrons, for the demonstration of electron vortices in [12], we developed electron-transparent gratings. The patterned silicon nitride gratings used for much of our research work by modulating the *phase* of an illuminating plane wave, rather than modulating the *amplitude* of a wave by removing parts of the beam (scattering or absorbing electrons). Several groups are now independently optimizing the depth and shape profile of the grooves milled into these electron-transparent membranes in order to maximize the beam current in a desired diffraction order [52–55]. Non-relativistic electrons propagating through the material membrane acquire a phase $\phi = eVL/v\hbar$, where V is the mean inner potential of the membrane, L is the projected thickness and v is the electron's velocity. Thus, varying the thickness of the grating as a function of position allows one to modulate the phase of the electron wave. For silicon nitride patterned with FIB, we find that a thickness modulation ΔL of 30–40 nm is enough to modulate the phase of a 300 keV electron by π radians. We have successfully made blazed gratings that place over 70% of the incident beam current into a diffraction order, and sinusoidal gratings that suppress the 0-order and place 30% of the incident beam current in each of the $+1$ and -1 diffraction orders.

While a digitally reconfigurable hologram such as a spatial light modulator (SLM) does not yet exist for electron beams, several different nanofabricated holograms can be placed on a single silicon nitride membrane (see the electronic supplementary material). When installed as an aperture of a condenser lens in a TEM, this wafer with multiple holograms can be positioned such that only one grating at a time is illuminated by electrons. This provides versatility to conduct many different experiments with the same device, reducing the need to repeatedly vent the TEM.

3. Experiments and demonstrations of free electron vortices

(a) Production of electron beams with orbital angular momentum from diffraction holograms

Figure 5 presents a TEM electron diffraction experiment using the grating shown in figure 4. At 80 keV ($\lambda = 4.18$ pm), electron beams diffracted from this grating had a free space angular spread of only 50 µrad. However, the strength of the TEM imaging system was employed to magnify this angular separation to observe the diffracted waves in the far field regime (Fraunhofer approximation), such that the diffraction spots could be resolved when projected onto the imaging detector.

Experimental results such as those shown in figures 5 indicate that low-OAM states for electron vortex beams appear to be stable. That is, despite the rest mass and charge of the electron wave function, these states do not appear to radiate or decay upon propagation through free space and their spiral phase is maintained. These states are stable even to higher OAM. As shown in figures 6 and 7 there appears to be no limit to the amount of OAM that can be imparted to an electron wave function. While focal series show that these high OAM ring-shaped distributions retain their OAM, imperfections in the electron optics result in the elliptic distortions of the beams, as can be seen in figure 7. More fundamentally, these distortions should result in the breakup of the high-order vortex into a cluster of many charge-1 singularities [56,57].

(b) Measuring the spiral phase of electron orbital angular momentum beams

As discussed in [12], the use of electron-transparent phase gratings provides a convenient way to characterize the wavefront of the diffracted beams. Figure 8*a* shows the results of a simple,

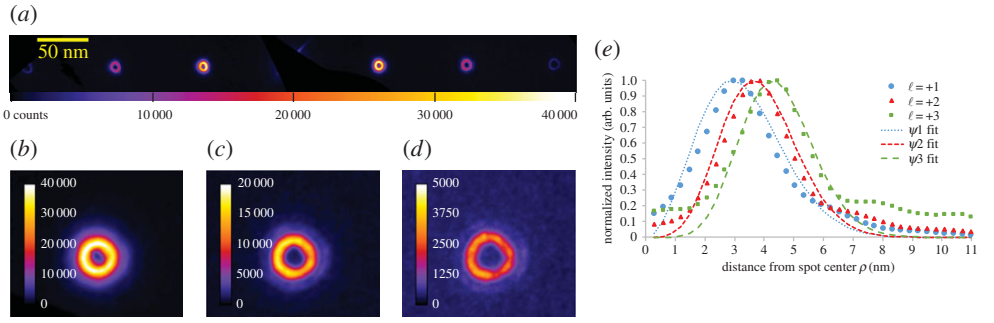

Figure 5. (*a*) A TEM image of the 80 keV electrons diffracted from the grating in figure 4. The central order has been removed by a beam block. A colour scale is used for this and subsequent images of diffraction patterns in order to make less intense features visible. (*b–d*) Magnified images of the +1, +2 and +3 diffraction orders. (*e*) Azimuthally averaged radial profiles of each of these diffracted beams reveals the dependence of the vortex core size on the topological charge. The dashed lines are fits derived from a Laguerre–Gaussian model of the electron wave functions (equation (4.1)).

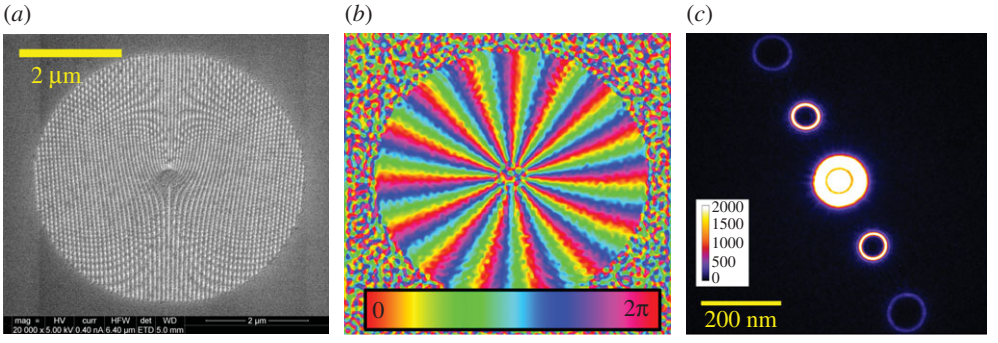

Figure 6. (*a*) An SEM micrograph image of a nanofabricated silicon nitride diffraction hologram with 15 extra grooves for producing electron beams with high OAM. (*b*) The $\ell = 15$ phase topology encoded in the hologram can be revealed by Fourier-filtering the SEM micrograph image. (*c*) TEM images of an actual electron diffraction pattern (300 keV) show electron vortex beams with multiples of 15$\hbar$ units of OAM.

single-grating electron interferometry experiment in which a wide electron beam coherently illuminates a forked grating and a large area of the transparent membrane surrounding it. The portion of the electron wave function that is transmitted through the unpatterned membrane serves as a reference wave, and at intermediate values of TEM defocus this overlaps the diffracted beams emanating from the grating. The interference between a helical electron wavefront and a flat wavefront is shown in figure 8*a*. The fork dislocation predicted [17,18] and first measured [10] by Tonomura & Uchida is visible in the interferogram. A holographic reconstruction of these fringes, shown in figure 8*b*, makes the spiral phase topology of the diffracted beams quite evident.

In most ways, free electron wave functions possessing OAM behave just like twisted light. The dark node in the centre of the electron vortex beam remains there under propagation through free space—even throughout the Rayleigh range of a beam waist [12]—as described by the Laguerre–Gaussian wave function developed for optics (equation (4.1)). The evolution of optical OAM modes in astigmatic optical systems has been explored experimentally using cylindrical lenses, e.g. [58]. Likewise, electron OAM states transform similarly upon propagation through astigmatic optical systems [59–61]. In figure 9, electron OAM beams were propagated through a magnetic quadrupole lens, the electron-optical equivalent of a cylindrical lens. An electron vortex beam with topological charge 2 breaks up into two separate vortices. This can be used as a quick way

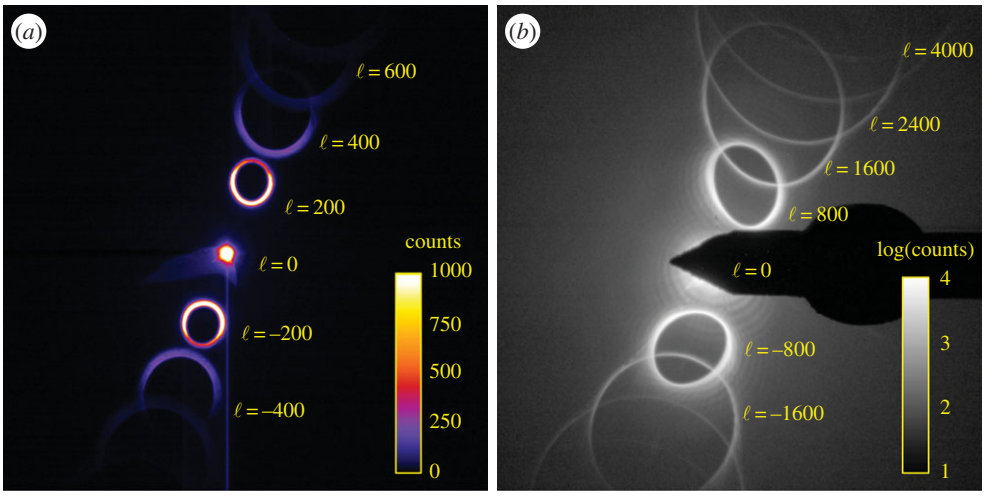

Figure 7. Electrons with extremely high OAM diffracted from a grating with topological charge of 200 (*a*) and 800 (*b*). A colour scale has been applied to (*a*) to make higher orders visible. For (*b*), the 0th-order beam has been removed by a beam block and a log scale applied to the image to make lower intensity, higher diffraction orders with extremely high amounts of OAM visible in the image. Electrons with 4000$\hbar$ are visible. Such beams are very sensitive to imperfections in the electron optics, and any small leftover astigmatism results in elliptic distortions seen here.

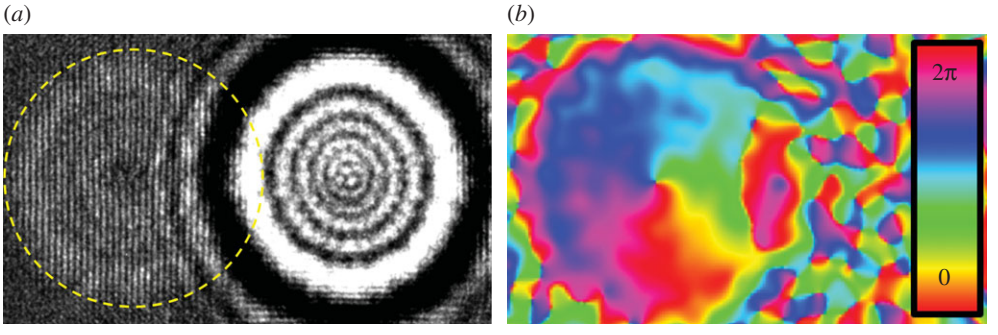

Figure 8. Electron interferometry reveals the spiral phase topology imprinted onto electron vortex beams diffracted from the grating shown in figure 4. (*a*) An intermediate-field (far-defocus) TEM image of the grating reveals interference between the diffracted wave (circled in dashed yellow) and a reference wave directly transmitted through the surrounding transparent membrane, as discussed in [12]. The brighter concentric circular pattern on the right is the undiffracted 0-order of the grating. (*b*) Holographic phase reconstruction of the interferogram confirms the spiral phase of the diffracted beam.

to characterize the OAM of the electron beam [61,63]. Schattschneider *et al.* [62] used this mode conversion to prepare electron vortex beams.

Unlike the case for light, isolation of inelastically scattered electrons can be challenging, so non-interferometric methods to measure OAM may be necessary for inelastic scattering experiments with electron vortex beams. Three different non-interferometric methods have been demonstrated: diffraction grating-based phase flattening [63,64], measurements using apertures [63] and mode transformation with cylindrical lenses [61,63], yet none of these techniques are suitable for measuring *mixtures* of OAM in scattered electrons. Two new proposed techniques for *sorting* electrons based on OAM include magnetic lens-based on-axis sorting [65], and electrostatic off-axis sorting [66,67]. The latter is inspired by optical OAM sorters [58].

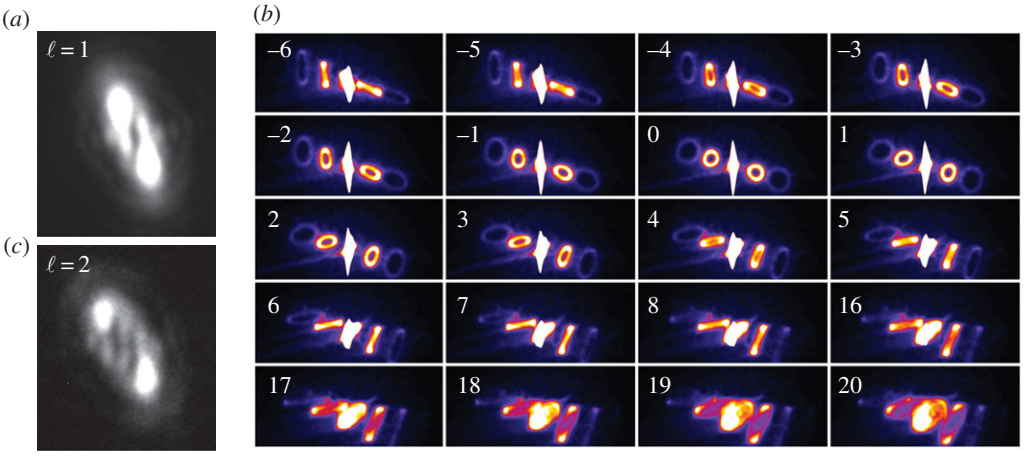

Figure 9. Transformation of electron OAM states within astigmatic electron optical systems. A magnetic quadrupole can be used to introduce the astigmatic perturbation to vortex beams, useful for mode conversion [62]. The central dark spot of a single topological charge state distorts into an edge-type phase dislocation, forming a dark line across the spot (*a*). (*c*) A series of images of astigmatic higher OAM states shows that each state becomes an ellipse. The numbers in each image of this sequence denote the astigmatism (expressed in scaled instrumental units) introduced by tuning the field gradient of a magnetic quadrupole lens (the diffraction stigmator on the TEM). One can see that negative OAM states on the left side of the diffraction pattern are all tilted in different directions from those on the right. The evolution of each OAM state is reminiscent of a current loop precessing in space. At high enough quadrupole excitation (lower rightmost image), the OAM states seem to have inverted.

4. Modelling free electron vortices

Free electron vortex states can be visualized and formally modelled in several ways. Just as with all quantum vortices, the electron vortex wave function is defined by an azimuthal phase, $\exp(\mathrm{i}\ell\phi)$, where the integer ℓ is the topological charge, or winding number, defining the spiral phase singularity. The corresponding OAM of the electron about an axis parallel to the vortex core (defined here as the optical axis in the $+z$ direction) is equal to the topological charge times Planck's constant, $L_z = \ell\hbar$. Unlike quantum vortices in bound systems, however, free electron vortices have characteristic dimensions that evolve in space and time, as generally described by the Dirac equation [27,31]. The Schrödinger wave equation can appropriately be used to model non-relativistic free electron vortex evolution in most TEM experiments [68].

(a) A convenient model for paraxial electron orbital angular momentum wave functions

A Laguerre–Gaussian beam with no radial modes ($p = 0$) provides a convenient, simple model of the electron vortex wave function ψ_ℓ. It describes the evolving width, wavefront curvature, and phase of electron wave functions in an electron microscope:

$$\psi_\ell(\rho,\phi,z,t) = \frac{A_\ell}{w(z)}\left(\frac{\sqrt{2}\rho}{w(z)}\right)^{|\ell|}\exp\left(\frac{-\rho^2}{w(z)^2}\right)\mathrm{e}^{-\mathrm{i}\omega t}\,\mathrm{e}^{\mathrm{i}\Phi_\ell(\rho,\phi,z)}, \tag{4.1a}$$

where A_ℓ is a normalization constant such that $\int|\psi_\ell(\rho,\phi,z)|^2\,\mathrm{d}\boldsymbol{r} = 1$, $\omega = E/\hbar$ is the temporal frequency related to the electron's energy and the characteristic transverse size of the wave function, $w(z)$, evolves upon propagation according to standard Gaussian optics. The spatial phase Φ_ℓ of this wave function is

$$\Phi_\ell(\rho,\phi,z) = kz + \ell\phi + \frac{k\rho^2}{2R(z)} - (|\ell|+1)\arctan(z/z_R) + \varphi_\ell, \tag{4.1b}$$

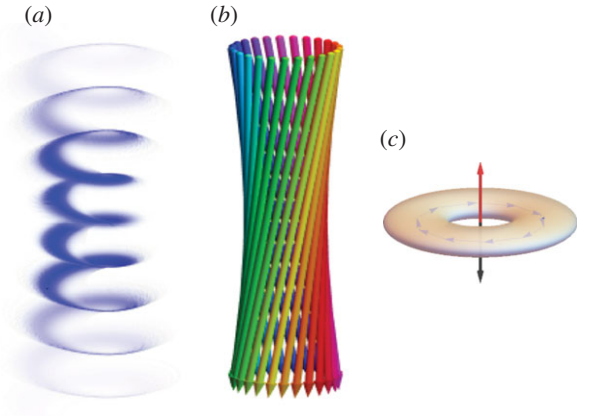

Figure 10. Representations of an electron vortex wavepacket. (*a*) A Laguerre–Gaussian wave function serves as a model for electron de Broglie wavepackets in a focused electron vortex beam. The helical wavefront is plotted as a surface of constant phase, with an opacity is proportional to $|\psi_\ell(\rho,\phi,z)|^2$, the probability distribution of the wave function. (*b*) A geometric model of the beam can be derived by evaluating the local momentum of the Laguerre–Gaussian function. Here, the probability current evaluated at the radius of peak amplitude of the wave function forms a collection of skewed straight rays. (*c*) In the centre-of-mass (CM) frame of reference, the circulating electron vortex probability distribution is torus-shaped, depicted here as a surface of constant probability. The quantized OAM, L_z, about the toroid centre (black arrow) combined with the electron's charge gives rise to an associated magnetic moment μ_ℓ (red arrow) described by equation (4.2). In this CM frame, both the transverse width of the doughnut, determined by the width of the beam, and the longitudinal extent of the torus along z, related to the spread in longitudinal momentum, evolve in time.

where $R(z)$ is the radius of wavefront curvature. For generality, φ_ℓ is a phase that can be introduced by interactions with external parameters that depend on the topological charge. When describing propagation through free space, $\varphi_\ell = 0$.

Equation (4.1) can be used to visualize the electron vortex wave function as a surface of constant phase. In figure 10*a*, such a wavefront is plotted as a parametric surfaces defined by $r(\rho,z) = (\rho\cos\phi(\rho,z), \rho\sin\phi(\rho,z), z)$, where $\phi(\rho,z)$ is provided by setting Φ_ℓ in equation (4.1*b*) equal to an integer multiple of 2π. In this visualization, the amplitude of the wave (the modulus of equation (4.1*a*)) is represented by the shading and opacity of the surface. A wave function model of freely propagating electron OAM states, such as equation (4.1), can be applied to understand the scattering of these states from other systems, or their dynamics in external fields.

A ray model of the free electron vortex OAM state above can be derived by considering the local charge current density of the wave function above. The charge current density associated with this wave function is given by $\boldsymbol{j}(\boldsymbol{r},t) = (-\mathrm{i}e\hbar/2m_e)(\psi^*\nabla\psi - \psi\nabla\psi^*)$. Berry & McDonald [69] performed an identical calculation of the local momentum distribution of an optical vortex. They found that while the energy flow lines within an optical vortex wave function can curl around the optical axis in the evanescent regions of a Laguerre–Gaussian beam, the flow lines become simple straight rays at the locations of peak probability in the beam. A similar interpretation of optical vortex beams was provided in [70]. A geometric model of charged particles following skewed, straight trajectories in space (figure 10*b*) offers practical benefits in visualization and simulations.

Note that in a reference frame co-propagating with the electron centre-of-mass, the electron vortex probability distribution can be visualized as a toroidal cloud of charge, with a longitudinal extent determined by the energy spread along the axis (figure 10*c*). This donut-shaped electron cloud rotates, and as it does so it expands in free space (or contracts, if initially given a negative radial momentum by a lens). A simple model of the free electron vortex as a loop of charged current can serve as a useful tool to understand how these states interact with and evolve in magnetic fields, as will be discussed in the following section.

(b) Free electron vortices in a magnetic field

Unlike photon OAM, the electron is a charged particle, and so the quantized OAM of the electron vortex state has an associated magnetic dipole moment. This magnetic moment is different from the intrinsic magnetic moment due to the electron's spin. The size and direction of an electron vortex magnetic moment μ_ℓ can be calculated from the charge current density using the formula $\boldsymbol{\mu}_\ell = \frac{1}{2}\int \boldsymbol{r} \times \boldsymbol{j}\, \mathrm{d}\boldsymbol{r}$. The azimuthal term of the cross product:

$$\mu_\ell = \frac{-\mathrm{i}e\hbar}{4m_e}\int_0^\infty \int_0^{2\pi} \left[\psi_\ell{}^* \left(\frac{1}{\rho}\frac{\partial \psi_\ell}{\partial \phi}\right) - \psi_\ell \left(\frac{1}{\rho}\frac{\partial \psi_\ell{}^*}{\partial \phi}\right)\right] \rho^2\, \mathrm{d}\phi\, \mathrm{d}\rho. \tag{4.2}$$

Inserting equation (4.1), we find that each electron vortex wave function possesses an orbital magnetic moment equal to $\mu_\ell = -e\hbar\ell/2m_e$. This serves as another example that all magnetic phenomenon arise from the angular momentum of electrical charges.

We can generally express the magnetic moment of any electronic state as $\mu_\ell = -g\mu_B\ell$ where $\mu_B = e\hbar/2m_e$ is the Bohr magneton and g is the gyromagnetic ratio. In deriving equation (4.2), we have shown that $g = 1$ for the specific case of a Laguerre–Gaussian electron vortex wave function, as is the case for well-defined orbital states in bound electron systems. Gallatin & McMorran [31] used this to show that because the gyromagnetic ration $g = 1$, in an external magnetic field the orbital axis (and orbital magnetic moment) of an electron vortex wave function will precess. However, the magnetic moment of the vortex state precesses at a different rate in the magnetic field compared to the classical orbital motion of the centre of mass. That is, the Larmor precession frequency of the orbital magnetic moment is half of the cyclotron frequency.

An unpolarized electron vortex state possessing OAM propagating along an external magnetic field acquires a longitudinal phase shift. A simplistic derivation can be provided by the Hamiltonian

$$H = H_0 + U,$$

where H_0 is the unperturbed Hamiltonian of the electron and U is the Zeeman interaction energy of the electron vortex orbital magnetic moment with the external field:

$$U = -\boldsymbol{\mu}_\ell \cdot \mathbf{B} = \frac{e\hbar\ell B}{2m_e}.$$

Using the WKB approximation, it is seen that this interaction leads to a field-dependent phase shift of the electron wave function:

$$\varphi_\ell = \frac{U\Delta t}{\hbar} = \frac{U\Delta z}{\hbar v} = \frac{e\ell B\Delta z}{2m_e v} = \frac{e\ell B\Delta z\lambda}{2h},$$

where we have ignored higher-order effects such as fringing fields, relativistic corrections and modifications to the transverse kinetic energy. For a more rigorous derivation of this same phase shift, see Bliokh *et al.* [32].

The orbital magnetic moment of the electron vortex state interacts in unique ways with an external magnetic field, for example, inducing rotations in superpositions of OAM in a longitudinal field [32,33,71], and OAM precession in a transverse field [31]. The kinetic angular momentum of the beam can also vary as the electron vortex beam propagates in a uniform longitudinal magnetic field, although *canonical* angular momentum remains constant [34,72]. Electron spin angular momentum (SAM) can couple to OAM in non-uniform magnetic and electric fields [73], which may open a new path to producing spin-polarized electrons [74]. Further experimental research in this area is likely to provide insight into fundamental electron physics, magnetism and electron microscopy.

5. Applications for electron beams with orbital angular momentum

Applications for engineered phase singularities such as optical vortices have been developed for optical imaging, communications, quantum optics and micro-manipulation for over two decades. The many applications of optical vortices developed for light microscopy, such as spiral phase microscopy [75], are generating a surge of interest within the electron microscopy community, with hopes that electronic analogues to these techniques might be developed. For example, as in optical microscopy, spiral phase electron microscopy can provide new information about phase objects at the nanoscale [76].

Under certain conditions, electron vortex beams can transfer OAM to matter at very small length scales [35–39,77]. For example, angular momentum-exchanging inelastic interactions between electron vortex probes and core-shell excitations in atoms could provide signals akin to magnetic circular dichroism of X-rays, albeit on a much finer length scale [35–37]. The promise of this electron magnetic helical dichroism signal is that it could be used to map individual magnetic moments at the atomic scale [78]. However, this signal is extremely sensitive to spatial overlap between the electron vortex probe and the atom's electronic states, so an aberration-corrected, sub-ångström probe is necessary [35]. It should be noted that to achieve these conditions for efficient electron OAM transfer to a single atom within a specimen, the specimen must sit in a high magnetic field of the electron microscope's objective lens, which typically exceeds 1.5 T. Further difficulties in this work include limiting the change in OAM during elastic propagation of a vortex through a crystal and accounting for the effects of probe coherence [35, 79,80]. Yet several research groups are currently tackling these issues, and a demonstration of using electron vortices to probe angular momentum at atomic dimensions may not be far off.

6. Conclusion

In 1992, Allen *et al.* revolutionized the world of optics by showing that light can occupy quantized orbital states, spawning many discoveries in the quarter century since. Recently, several groups showed that Allen *et al.*'s result applies to electron wave functions and other matter waves, too. Thus, optical OAM is a general property of all wave functions propagating in free space. These recent results underline how the Allen *et al.* paper brings new life to a 175 year old idea in physics: the topology and angular momentum of vortex structures provides a convenient model for many fundamental effects in low-energy physics. The advent of electron vortex beams shows that OAM is a new degree of freedom for free electrons that can lead to new interactions with matter and fields. Electron OAM is generating growing interest in the electron microscopy community as a new way to probe chirality and angular momentum at the nanoscale.

Data accessibility. Raw data files consist primarily of TEM images in the DM3 format, and are available upon request to the corresponding author.

Authors' contributions. B.J.M. conceived of and designed the study, performed experiments and data analysis, and drafted the manuscript. A.A. and J.S.P. fabricated the diffraction holograms. P.A.E. and M.L. carried out experiments in figures 2, 4 and 7, A.A.H. carried out experiments in figure 5 and 8, V.G. and T.R.H. carried out experiments in figure 7. All authors read and approved the manuscript.

Competing interests. We declare we have no competing interests.

Funding. This work at UO was supported by the U.S. Department of Energy, Office of Science, Basic Energy Sciences, under award no. DE-SC0010466. A.A. acknowledges support under the Cooperative Research Agreement between the University of Maryland and the National Institute of Standards and Technology, Center for Nanoscale Science and Technology, award no. 70NANB10H193, through the University of Maryland

Acknowledgements. The authors are grateful to Grant Baumgardner (ASU) for help fabricating the first forked diffraction grating for electrons, to Henri Lezec (NIST) for guidance on FIB nanofabrication, to Mark Stiles (NIST) and Gregg Gallatin (formerly NIST) for discussions related to theoretical interpretations of electron vortex states, to Charles Clark (NIST/JQI) for discussions related to J. J. Thomson's early work on the vortex model of matter, and to Ian Anderson (formerly NIST) for guidance on TEM. The author gratefully

acknowledges the use of UO CAMCOR facilities, which have been purchased with a combination of federal and state funding.

References

1. Allen L, Beijersbergen MW, Spreeuw RJC, Woerdman JP. 1992 Orbital angular momentum of light and the transformation of Laguerre-Gaussian laser modes. *Phys. Rev. A* **45**, 8185. (doi:10.1103/PhysRevA.45.8185)
2. Whewell W. 1833 Essay towards a first approximation to a map of cotidal lines. *Phil. Trans. R. Soc. Lond.* **123**, 147–236. (doi:10.1098/rstl.1833.0013)
3. Whewell W. 1836 On the results of an extensive system of tide observations made on the coasts of Europe and America in June 1835. *Phil. Trans. R. Soc. Lond.* **126**, 289–341. (doi:10.1098/rstl.1836.0019)
4. Berry MV. 1981 Singularities in waves and rays. In Lecture series session, no. 35 (ed. Les Houches), pp. 453–543. Amsterdam, The Netherlands: North-Holland.
5. Berry MV. 2002 Exuberant interference: rainbows, tides, edges, (de)coherence. *Phil. Trans. R. Soc. Lond. A* **360**, 1023–1037. (doi:10.1098/rsta.2001.0979)
6. Rankine WJM. 1851 On the centrifugal theory of elasticity, as applied to gases and vapours. *Philos. Mag.* **2**, 509–542.
7. Thomson W. 1869 On vortex atoms. *Proc. R. Soc. Edinb.* **6**, 94–105. (doi:10.1017/S0370164600045430)
8. Thomson JJ. 1883 *A treatise on the motion of vortex rings*. London, UK: MacMillan.
9. Thomson JJ. 1967 1906 Nobel lecture: carriers of negative electricity. In *Nobel lectures, physics 1901–1921*. Amsterdam, The Netherlands: Elsevier Publishing Company.
10. Uchida M, Tonomura A. 2010 Generation of electron beams carrying orbital angular momentum. *Nature* **464**, 737–739. (doi:10.1038/nature08904)
11. Verbeeck J, Tian H, Schattschneider P. 2010 Production and application of electron vortex beams. *Nature* **467**, 301–304. (doi:10.1038/nature09366)
12. McMorran BJ, Agrawal A, Anderson IM, Herzing AA, Lezec HJ, McClelland JJ, Unguris J. 2011 Electron vortex beams with high quanta of orbital angular momentum. *Science* **331**, 192–195. (doi:10.1126/science.1198804)
13. Thomson GP, Reid A. 1927 Diffraction of cathode rays by a thin film. *Nature* **119**, 890–890. (doi:10.1038/119890a0)
14. Thomson GP. 1965 1935 Nobel lecture: electronic waves. In *Nobel lectures, physics 1922–1941*. Amsterdam, The Netherlands: Elsevier Publishing Company.
15. Dirac PAM. 1931 Quantised singularities in the electromagnetic field. *Proc. R. Soc. Lond. A* **133**, 60–72. (doi:10.1098/rspa.1931.0130)
16. Dirac PAM. 1948 The theory of magnetic poles. *Phys. Rev.* **74**, 817. (doi:10.1103/PhysRev.74.817)
17. Fukuhara A, Shinagawa K, Tonomura A, Fujiwara H. 1983 Electron holography and magnetic specimens. *Phys. Rev. B* **27**, 1839–1843. (doi:10.1103/PhysRevB.27.1839)
18. Tonomura A. 1987 Applications of electron holography. *Rev. Mod. Phys.* **59**, 639–669. (doi:10.1103/RevModPhys.59.639)
19. Vinen WF. 1961 The detection of single quanta of circulation in liquid helium II. *Proc. R. Soc. Lond. A* **260**, 218–236. (doi:10.1098/rspa.1961.0029)
20. Blatter G, Feigel'man MV, Geshkenbein VB, Larkin AI, Vinokur VM. 1994 Vortices in high-temperature superconductors. *Rev. Mod. Phys.* **66**, 1125–1388. (doi:10.1103/RevModPhys.66.1125)
21. Matthews MR, Anderson BP, Haljan PC, Hall DS, Wieman CE, Cornell EA. 1999 Vortices in a Bose-Einstein condensate. *Phys. Rev. Lett.* **83**, 2498–2501. (doi:10.1103/PhysRevLett.83.2498)
22. Hirschfelder JO, Christoph AC, Palke WE. 1974 Quantum mechanical streamlines. I. Square potential barrier. *J. Chem. Phys.* **61**, 5435–5455. (doi:10.1063/1.1681899)
23. Hirschfelder JO, Goebel CJ, Bruch LW. 1974 Quantized vortices around wavefunction nodes. II. *J. Chem. Phys.* **61**, 5456–5459. (doi:10.1063/1.1681900)
24. Nye JF, Berry MV. 1974 Dislocations in wave trains. *Proc. R. Soc. Lond. A* **336**, 165–190. (doi:10.1098/rspa.1974.0012)

25. Berry MV. 1980 Exact Aharonov-Bohm wavefunction obtained by applying Dirac's magnetic phase factor. *Eur. J. Phys.* **1**, 240. (doi:10.1088/0143-0807/1/4/011)
26. Bialynicki-Birula I, Bialynicka-Birula Z. 2000 Motion of vortex lines in quantum mechanics. *Phys. Rev. A* **61**, 32110. (doi:10.1103/PhysRevA.61.032110)
27. Bliokh K, Bliokh Y, Savel'ev S, Nori F. 2007 Semiclassical dynamics of electron wave packet states with phase vortices. *Phys. Rev. Lett.* **99**, 190404. (doi:10.1103/PhysRevLett.99.190404)
28. Willis BTM. 1957 An optical method of studying the diffraction from imperfect crystals. II. crystals with dislocations. *Proc. R. Soc. Lond. A* **239**, 192–201. (doi:10.1098/rspa.1957.0032)
29. Suzuki T, Willis BTM. 1956 Diffraction from dislocations. *Nature* **177**, 712. (doi:10.1038/177712a0)
30. McMorran BJ. 2009 Electron diffraction and interferometry using nanostructures PhD dissertation, University of Arizona, Tucson, AZ.
31. Gallatin GM, McMorran B. 2012 Propagation of vortex electron wave functions in a magnetic field. *Phys. Rev. A* **86**, 012701. (doi:10.1103/PhysRevA.86.012701)
32. Bliokh KY, Schattschneider P, Verbeeck J, Nori F. 2012 Electron vortex beams in a magnetic field: a new twist on landau levels and Aharonov-Bohm states. *Phys. Rev. X* **2**, 041011. (doi:10.1103/PhysRevX.2.041011)
33. Greenshields C, Stamps RL, Franke Arnold S. 2012 Faraday rotation for superpositions of electron vortex states. (http://arxiv.org/abs/1204.4698)
34. Babiker M, Yuan J, Lembessis VE. 2015 Electron vortex beams subject to static magnetic fields. *Phys. Rev. A* **91**, 013806. (doi:10.1103/PhysRevA.91.013806)
35. Idrobo JC, Pennycook SJ. 2011 Vortex beams for atomic resolution dichroism. *J. Electron Microsc.* **60**, 295–300.
36. Lloyd S, Babiker M, Yuan J. 2012 Quantized orbital angular momentum transfer and magnetic dichroism in the interaction of electron vortices with matter. *Phys. Rev. Lett.* **108**, 074802. (doi:10.1103/PhysRevLett.108.074802)
37. Schattschneider P, Schaffer B, Ennen I, Verbeeck J. 2012 Mapping spin-polarized transitions with atomic resolution. *Phys. Rev. B* **85**, 134422. (doi:10.1103/PhysRevB.85.134422)
38. Asenjo-Garcia A, Garcíade Abajo FJ. 2014 Dichroism in the interaction between vortex electron beams, plasmons, and molecules. *Phys. Rev. Lett.* **113**, 066102. (doi:10.1103/PhysRevLett.113.066102)
39. Harvey TR, Pierce JS, Chess JJ, McMorran BJ. 2015 Demonstration of electron helical dichroism as a local probe of chirality. (http://arxiv.org/abs/1507.01810)
40. Blackburn AM, Loudon JC. 2014 Vortex beam production and contrast enhancement from a magnetic spiral phase plate. *Ultramicroscopy* **136**, 127–143. (doi:10.1016/j.ultramic.2013.08.009)
41. Béché A, Van Boxem R, Van Tendeloo G, Verbeeck J. 2014 Magnetic monopole field exposed by electrons. *Nat. Phys.* **10**, 26–29.
42. Rajantie A. 2016 The search for magnetic monopoles. *Phys. Today* **69**, 40–46. (doi:10.1063/PT.3.3328)
43. Blackburn AM, Loudon JC, Herring R, Hrabec A, Hoyle D. 2015 At-focus observations of high quality electron vortex beams created from ferromagnetic rods. *Microsc. Microanal.* **21**, 501–502.
44. Béché A, Juchtmans R, Verbeeck J. In press. Efficient creation of electron vortex beams for high resolution STEM imaging. Ultramicroscopy. (doi:10.1016/j.ultramic.2016.05.006)
45. Gotte JB, Franke-Arnold S, Zambrini R, Barnett SM. 2007 Quantum formulation of fractional orbital angular momentum. *J. Mod. Opt.* **54**, 1723–1738. (doi:10.1080/09500340601156827)
46. Blackburn AM. 2016 Observation of an electron vortex beam created from a self-charging rod. *Microsc. Microanal.* **22**, 1710–1711.
47. Bazhenov VY, Vasnetsov MV, Soskin MS. 1990 Laser beams with screw dislocations in their wavefronts. *J. Exp. Theor. Phys. Lett.* **52**, 1037–1039.
48. Heckenberg NR, McDuff R, Smith CP, Rubinsztein-Dunlop H, Wegener MJ. 1992 Laser beams with phase singularities. *Opt. Quantum Electron.* **24**, S951–S962. (doi:10.1007/BF01588597)
49. Clark TW, Offer RF, Franke-Arnold S, Arnold AS, Radwell N. 2016 Comparison of beam generation techniques using a phase only spatial light modulator. *Opt. Express* **24**, 6249. (doi:10.1364/OE.24.006249)

50. Harvey TR, Brougher G, Langworthy K, McMorran BJ. 2013 Small-pitch electron diffraction Holograms patterned on inorganic resist with electron beam lithography. In *EIPBN Proc.*, Nashville, TN, *28–31 May*. Omnipress. (http://eipbn.omnibooksonline.com)
51. Pierce JS, Wright C, Harvey TR, McMorran BJ. 2014 Creation of high resolution electron diffraction gratings using FIB and E-Beam techniques. In *EIPBN Proceedings, 27–30 May*, pp. P08-06. Washington, DC.
52. Harvey TR, Pierce JS, Agrawal AK, Ercius P, Linck M, McMorran BJ. 2014 Efficient diffractive phase optics for electrons. *New J. Phys.* **16**, 093039. (doi:10.1088/1367-2630/16/9/093039)
53. Pierce JS, Harvey TR, Yahn TS, McMorran BJ. 2013 High efficiency electron diffractive optics. *Microsc. Microanal.* **19**, 1188–1189. (doi:10.1017/S1431927613007939)
54. Grillo V, Gazzadi GC, Karimi E, Mafakheri E, Boyd RW, Frabboni S. 2014 Highly efficient electron vortex beams generated by nanofabricated phase holograms. *Appl. Phys. Lett.* **104**, 043109. (doi:10.1063/1.4863564)
55. Shiloh R, Lereah Y, Lilach Y, Arie A. 2014 Sculpturing the electron wave function using nanoscale phase masks. *Ultramicroscopy* **144**, 26–31. (doi:10.1016/j.ultramic.2014.04.007)
56. Dennis MR. 2006 Rows of optical vortices from elliptically perturbing a high-order beam. *Opt. Lett.* **31**, 1325–1327. (doi:10.1364/OL.31.001325)
57. Berry MV. 2013 A note on superoscillations associated with Bessel beams. *J. Opt.* **15**, 044006. (doi:10.1088/2040-8978/15/4/044006)
58. Bekshaev AY, Soskin MS, Vasnetsov MV. 2004 Transformation of higher-order optical vortices upon focusing by an astigmatic lens. *Opt. Commun.* **241**, 237–247. (doi:10.1016/j.optcom.2004.07.023)
59. McMorran B, Agrawal A, Anderson I, Herzing A, Lezec H, McClelland J, Unguris J. 2011 Electron beams carrying quantized orbital angular momentum. In *Laser science. OSA technical digest*, pp. LWL1. San Jose, CA: Optical Society of America.
60. McMorran B, Agrawal A, Anderson IM, Herzing AA, Lezec H, McClelland JJ. 2011 Electron Laguerre-Gaussian beams. In *Quantum electronics and laser science conf. OSA technical digest* (*CD*), pp. QMA1. San Jose, CA: Optical Society of America.
61. Shiloh R, Tsur Y, Remez R, Lereah Y, Malomed BA, Shvedov V, Hnatovsky C, Krolikowski W, Arie A. 2015 Unveiling the orbital angular momentum and acceleration of electron beams. *Phys. Rev. Lett.* **114**, 096102. (doi:10.1103/PhysRevLett.114.096102)
62. Schattschneider P, Stöger-Pollach M, Verbeeck J. 2012 Novel vortex generator and mode converter for electron beams. *Phys. Rev. Lett.* **109**, 084801. (doi:10.1103/PhysRevLett.109.084801)
63. Guzzinati G, Clark L, Béché A, Verbeeck J. 2014 Measuring the orbital angular momentum of electron beams. *Phys. Rev. A* **89**, 025803. (doi:10.1103/PhysRevA.89.025803)
64. Saitoh K, Hasegawa Y, Hirakawa K, Tanaka N, Uchida M. 2013 Measuring the orbital angular momentum of electron vortex beams using a forked Grating. *Phys. Rev. Lett.* **111**, 074801. (doi:10.1103/PhysRevLett.111.074801)
65. Harvey TR, McMorran BJ. 2016 A Stern–Gerlach-like approach to electron orbital angular momentum measurement. (http://arxiv.org/abs/1606.03631)
66. McMorran BJ, Harvey TR, Lavery MPJ. 2016 Efficient sorting of free electron orbital angular momentum. (http://arxiv.org/abs/arXiv:1609.09124)
67. Grillo V, Tavabi AH, Venturi F, Larocque H, Balboni R, Gazzadi GC. 2016 Measuring an electron beam's orbital angular momentum spectrum. (http://arxiv.org/abs/1609.09129)
68. Schattschneider P, Verbeeck J. 2011 Theory of free electron vortices. *Ultramicroscopy* **111**, 1461–1468. (doi:10.1016/j.ultramic.2011.07.004)
69. Berry MV, McDonald KT. 2008 Exact and geometrical optics energy trajectories in twisted beams. *J. Opt. A Pure Appl. Opt.* **10**, 035005. (doi:10.1088/1464-4258/10/3/035005)
70. Volyar AV, Shvedov VG, Fadeeva TA. 1999 Rotation of the wavefront of an optical vortex in free space. *Tech. Phys. Lett.* **25**, 203–206. (doi:10.1134/1.1262423)
71. Guzzinati G, Schattschneider P, Bliokh KY, Nori F, Verbeeck J. 2013 Observation of the larmor and gouy rotations with electron vortex beams. *Phys. Rev. Lett.* **110**, 093601. (doi:10.1103/PhysRevLett.110.093601)
72. Greenshields CR, Stamps RL, FrankeArnold S, Barnett SM. 2014 Is the angular momentum of an electron conserved in a uniform magnetic field? *Phys. Rev. Lett.* **113**, 240404. (doi:10.1103/PhysRevLett.113.240404)

73. Karimi E, Marrucci L, Grillo V, Santamato E. 2012 Spin-to-orbital angular momentum conversion and spin-polarization filtering in electron beams. *Phys. Rev. Lett.* **108**, 044801. (doi:10.1103/PhysRevLett.108.044801)
74. Harris J, Grillo V, Mafakheri E, Gazzadi GC, Frabboni S, Boyd RW, Karimi E. 2015 Structured quantum waves. *Nat. Phys.* **11**, 629–634. (doi:10.1038/nphys3404)
75. Fürhapter S, Jesacher A, Bernet S, Ritsch-Marte M. 2005 Spiral phase contrast imaging in microscopy. *Opt. Express* **13**, 689–694. (doi:10.1364/OPEX.13.000689)
76. Juchtmans R, Clark L, Lubk A, Verbeeck J. 2016 Spiral phase plate contrast in optical and electron microscopy. *Phys. Rev. A* **94**, 023838. (doi:10.1103/PhysRevA.94.023838)
77. Xin HL, Zheng H. 2012 On-column 2p bound state with topological charge $+-1$ excited by an atomic-size vortex beam in an aberration-corrected scanning transmission electron microscope. *Microsc. Microanal.* **18**, 711–719. (doi:10.1017/S1431927612000499)
78. Idrobo JC, Rusz J, Spiegelberg J, McGuire MA, Symons CT, Vatsavai RR, Cantoni C, Lupini AR. 2016 Detecting magnetic ordering with atomic size electron probes. *Adv. Struct. Chem. Imaging* **2**, 5. (doi:10.1186/s40679-016-0019-9)
79. Rusz J, Bhowmick S. 2013 Boundaries for efficient use of electron vortex beams to measure magnetic properties. *Phys. Rev. Lett.* **111**, 105504. (doi:10.1103/PhysRevLett.111.105504)
80. Schattschneider P, Löffler S, Stöger-Pollach M, Verbeeck J. 2014 Is magnetic chiral dichroism feasible with electron vortices? *Ultramicroscopy* **136**, 81–85. (doi:10.1016/j.ultramic.2013.07.012)